Input-Output Synchronization for Bias Drift Reduction of MEMS Gyroscopes

Afshin Izadian, Jeremy Dawson, and Parviz Famouri, *Senior Member, IEEE*

Abstract—**MEMS vibratory gyroscopes ideally possess uncoupled components on their orthogonal drive and sense axes. Asymmetries in the structure of the device, caused by manufacturing non-idealities and device wear, introduce unwanted dynamic interactions between the sense and drive axes. These interactions often lead to the transfer of energy from the drive axis to the sense axis in the absence of any external perturbation. The transferred energy (leakage) appears as a time-accumulating bias drift on the measurement signal on the sense axis, resulting in error to the sensor output. This paper describes the application of an input-output controller to compensate for non-ideal interdependencies of drive and sense axes for vibratory gyroscopes in order to reduce the bias drift in the sense axis.**

I. INTRODUCTION

MEMS gyroscopes offer many advantages over their macro-mechanical counterparts, including low-power operation and the ability to accurately measure both high and low-amplitude angular velocities. The mechanical design of gyroscopes makes them robust to lateral vibrations [1]. The structure of MEMS gyroscopes ideally consists of two orthogonal axes known as drive and sense axes. Typically, a 'drive frame' is driven at resonance along the *x*-axis while its sensor frame proof mass (nested within the drive frame with sensitivity along the *y*-axis) remains stationary. In the presence of external rotation, a Coriolis force is generated, causing the vibrational energy of the drive frame to be transferred to the proof mass. The amount of energy transferred is proportional to the magnitude of the angular velocity. In an ideal structure, there is no motion of the proof mass in the absence of external rotation in the sensitivity plane of the frame of reference.

In real systems, due to imperfect manufacturing steps and environmental operating conditions, the drive and sense axes are interconnected by geometrical and material nonidealities, or defects, that create mutual dependencies between the axes. Anisoelasticity and anisoinertia are two of commonly known defects in MEMS gyros which result in spring constant and damping coefficient couplings on the sense and drive axes. To design functional devices, these terms must be considered in the device system equations. These defects result in false measurements even in the absence of external perturbation. The collective contribution of unwanted output due to structural nonidealities and other sources of system noise is known as bias drift [2].

Bias drift extensively degrades the output resolution of gyroscope and leads to accumulating error over time. Previous MEMS gyroscopes achieved high-resolution sensing by utilizing accurate and advanced micro fabrication processes. Xie and Fedder reported a device with $0.02^{\circ}/s/Hz^{1/2}$ with a sensitivity bandwidth of 5Hz [3]. Gyroscopes with wider bandwidth offer sensitivity to wider input frequency ranges at the cost of reduced gain for all frequencies [4].

Phenomena such as mechanical-thermal and electrical-thermal noise [5] [6], as well as environmental operating conditions, also contribute to device performance degradation. Compensation techniques such as force-balancing and adaptive controllers have been largely applied to identify and overcome these imperfections [1], [7]-[15]. However, very strong cross-axis interactions and the complex structure of MEMS gyroscopes make it very challenging to identify and accurately compensate for the coupled effects of these error sources. Some techniques utilize the adaptive control approach for frequency matching and phase-locking of the gyroscopes in sinusoidal trajectory tracking control that makes use of both velocity and displacement signals [17].

This paper presents a model-based input-output synchronizing technique for reducing sense axis measurement drift resulted from the mechanical structure imperfections. A model of a gyroscope without manufacturing imperfections is considered to generate the reference output. The plant's output (a gyro with imperfections) is synchronized to that of the model. The controller and its adaptation techniques provide faster and more accurate control at low adaptation gains without the need of any filter in the input and output signals of the gyroscope. The input-output control technique provides full synchronization of gyroscopes both in phase and amplitude.

II. MEMS GYROSCOPE PRINCIPLES

A vibratory MEMS gyroscope is shown in Figure 1 with orthogonal sense and drive axes and a proof mass which resonates along the sense axis. The orthogonal axes are modeled by second order mass spring damper systems with interdependent terms as [8]

Afshin Izadian is a PhD candidate at West Virginia University department of Computer Science and Electrical Engineering; e-mail: afshiniz@gmail.com

Jeremy Dawson is with West Virginia University, Morgantown WV. e-mail: Jeremy.dawson@mail.wvu.edu

Parviz Famouri is with department of Electrical Engineering at West Virginia University. e-mail: parviz.famouri@mail.wvu.edu

$$m\ddot{x}+d_{xx}\dot{x}+d_{xy}\dot{y}+(k_{xx}-m(\Omega_y^2+\Omega_z^2))x+(k_{xy}+m\Omega_x\Omega_y)y=f_x+2m\Omega_z\dot{y}$$
$$m\ddot{y}+d_{xy}\dot{x}+d_{yy}\dot{y}+(k_{yy}-m(\Omega_x^2+\Omega_z^2))y+(k_{xy}+m\Omega_x\Omega_y)x=f_y-2m\Omega_z\dot{x} \quad (1)$$

where m is the resonating mass along the drive (x) axis, k_{xx} and d_{xx} are spring constant and damping coefficients in the x direction respectively, and k_{yy}, d_{yy} are the sense-axis (y) dependent spring constant and damping coefficient values. The cross-axis coefficients representing the effect of manufacturing imperfections, and environmental conditions (on the sense and drive axes) are k_{xy} and d_{xy}. The values f_x, f_y are coupling forces on the drive and sense axes. Accordingly, the effect of any angular velocity Ω will have three components on x, y and z-directions expressed as $\Omega_x, \Omega_y, \Omega_z$. The Coriolis forces ($+2m\Omega_z\dot{y}$ and $-2m\Omega_z\dot{x}$) terms on the x and y-axes respectively are influenced only by the z-axis component of the angular velocity. Considering negligible values of Ω_x^2, Ω_y^2 and $\Omega_x.\Omega_y$, the system can be rewritten in reduced form as [8]

$$m\ddot{x}+d_{xx}\dot{x}+d_{xy}\dot{y}+k_{xx}x+k_{xy}y=f_x+2m\Omega_z\dot{y}$$
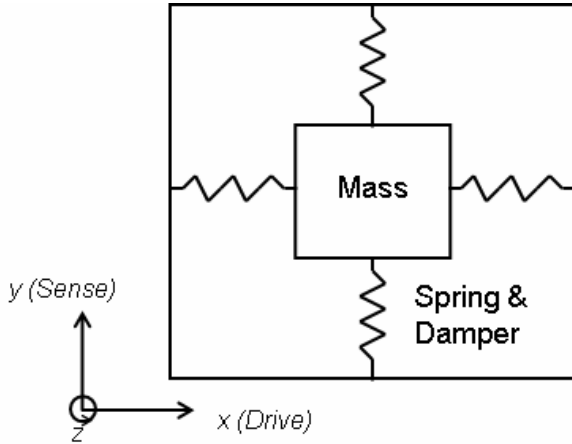$$m\ddot{y}+d_{xy}\dot{x}+d_{yy}\dot{y}+k_{yx}x+k_{yy}y=f_y-2m\Omega_z\dot{x} \quad (2)$$

Cross-axis coefficients resulting from anisoelasticity and anisoinertia are represented in the form of damping coefficient and spring constant interdependencies, which are both functions of the rotation angle of the respective damping and elastic axes away from the ideal axes. Anisoinertia is modeled by rotation angle α, which causes a spring constant variation as

$$k_{xx}=k_1\cos^2\alpha+k_2\sin^2\alpha$$
$$k_{yx}=(k_1-k_2)\sin\alpha\cos\alpha \quad , \quad (3)$$
$$k_{yy}=k_1\sin^2\alpha+k_2\cos^2\alpha$$

where k_1 and k_2 are the original spring constant along drive and

sense axes respectively. Considering the same rotation angle for damping coefficients by angle γ, the x-y cross-axis damping coefficients are expressed as

$$d_{xx}=d_1\cos^2\gamma+d_2\sin^2\gamma$$
$$d_{yx}=(d_1-d_2)\sin\gamma\cos\gamma \quad , \quad (4)$$
$$d_{yy}=d_1\sin^2\gamma+d_2\cos^2\gamma$$

where d_1 and d_2 are the original damping coefficients along the drive and sense axes respectively.

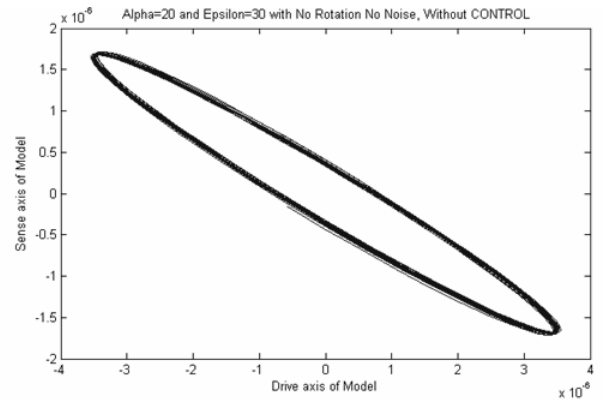With rotation angles of $\alpha=20$ and $\gamma=30$ degrees, the sense-drive axes locus is shown in Figure 2.

Fig. 2. Energy transferring from drive to sense axis. Dependencies are shown in case of 20 and 30 degrees on uncertainty.

III. INPUT-OUTPUT CONTROL APPROACH

In this section, a model based input-output control approach is applied for the MEMS gyroscopes to synchronize their phase and amplitude with an ideal structure. The control law and its gain adaptation technique are introduced for gyros. The control law (f_y) which is applied to the sense axis of the plant is expressed as

$$f_y=k_r y_m+k_e(y_p-y_m)+k_p r, \quad (5)$$

where k_r, k_e, k_p are controller coefficients. These values are estimated in order to match the output of plant (non-ideal gyro) with an ideal structure (model). The variables y_m, y_p are the reference model and plant's output signals, and r is the reference input to the model. In perfect matching control, the control coefficients k_r, k_e, k_p are found such that the output error between the model and plant becomes zero.

The switching hypersurface (s) is defined to satisfy the switching equation $s=Ge=0$, where G is the switching-gain matrix and $e=y_p-y_m$ is the tracking error.

Considering estimations of the coefficients as $\hat{k}_r, \hat{k}_e, \hat{k}_p$, the equivalent control command f_{yeq} is defined as

$$f_{yeq} = \hat{k}_r y_r + \hat{k}_e e + \hat{k}_p r \,. \tag{6}$$

Controller coefficients are computed according to the gain adaptation technique as

$$\dot{\hat{k}}_r = -P_0 \, \mathrm{sgn}(s) r \,, \tag{7}$$

$$\dot{\hat{k}}_P = -P_0 \, \mathrm{sgn}(s) y_p \,, \tag{8}$$

$$\dot{\hat{k}}_e = -P_0 \, \mathrm{sgn}(s) e \,. \tag{9}$$

∎

For interested readers, the stability proof of the controller is provided in [16].

Figure 3 shows the control system configuration with two gyros including an ideal gyro (model) and an imperfect fabricated device (plant) with rotation angles 4 and 5 degrees on damping and elasticity with respect to the ideal axes. The controller synchronizes the output of the plant with that of the model and compensates for non-idealities in the device to reduce the bias drift.
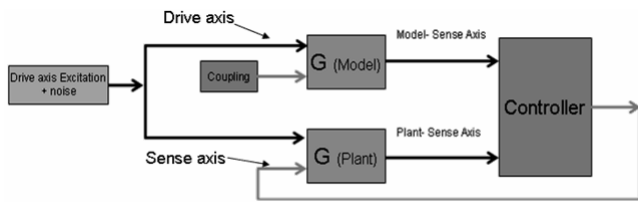

Fig. 3. Control configuration, the sense axis synchronization.

IV. SIMULATION RESULTS

As mentioned earlier, imperfect structure of MEMS gyroscopes causes unwanted energy-transfer from the drive to sense axis. Hence, the sensed output signal drifts from the true signal over time. Control of the output with its reference compensates for imperfections and enables accurate measurement of rotation and angular velocity. In the control scheme of this paper, the control command is applied to the force rebalancing fingers manufactured on the sense axis of the device. The amplitude of rebalancing force in small imperfections allows high drift reduction in the device.

After applying the control command with adaptation techniques, the synchronization profile shown in Figures 4 and 5 is achieved. Figure 4 shows the deviation and drift of the plant output from the desired signal before any control is applied to the system. Figure 5 shows the synchronization profile of the output after the control command is applied. The input-output control synchronizes the waveforms and compensates for the energy transfer caused by asymmetries in the device.

Figure 6 shows the locus of ideal model with a flat profile and zero interdependencies on the drive and sense axes. The plant (in this case, having 4 and 5 degrees of pattern rotation) had a non-ideal locus, causing deviation from the flat line profile. During control and synchronization, the locus of the gyro is forced to follow the same path (reference). Figure 7 shows the synchronization performance after 0.09 seconds. Tracking error theoretically reaches zero as time increases, providing a perfect tracking profile.
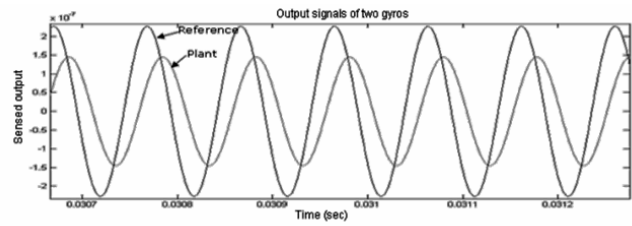

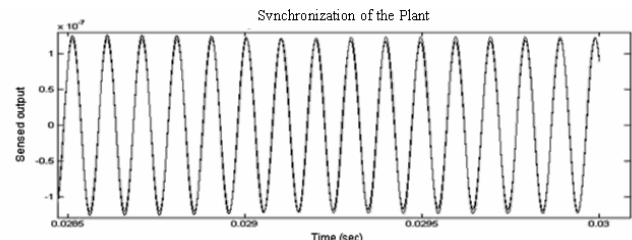Fig. 4. Sense axis output of two gyroscopes without controls.

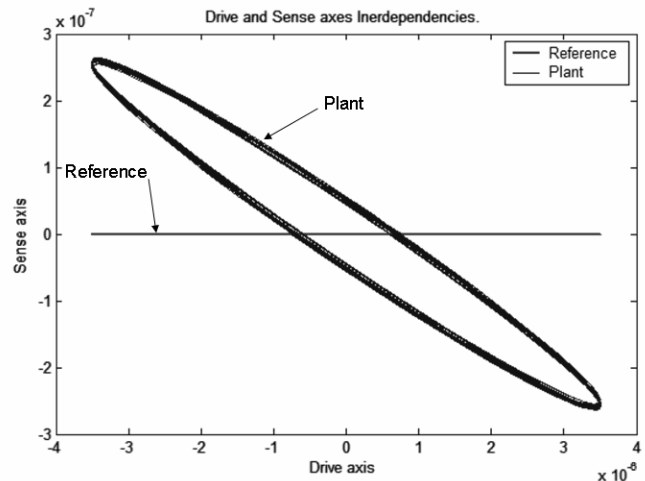Fig. 5. Sense axis output of two gyros after synchronization.

Fig. 6. Loci of Model and plant with pattern rotation on damping coefficient and spring constant before synchronization

The rebalancing force is generated by a fixed number of comb fingers designed and manufactured to compensate for the small imperfections on the sense axis of the device (plant). The controller generates force up to 5e-7N to synchronize the plant with the model. The compensating force is a small portion of the drive force and the comb resonator fingers designed for this purpose can compensate for small mechanical imperfections.
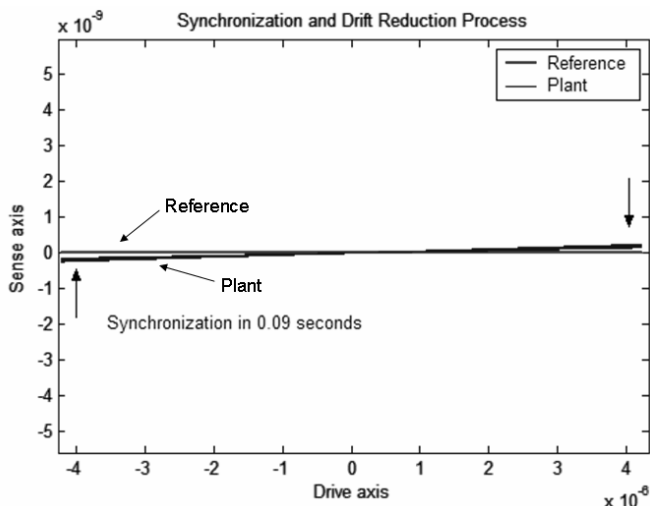
Fig. 7. Loci of Model and plant after synchronization. Synchronization time is about 0.09 seconds. The adaptation continues until reaching zero-error conditions.

Figure 8 shows the rebalancing force generated by the controller. It is seen that the force ideally compensates for the energy transferred from the drive axis to the sense axis due to non-ideal structure of the device. Higher imperfections in the form of higher rotation angles require stronger control efforts and a higher number of corrective force fingers.
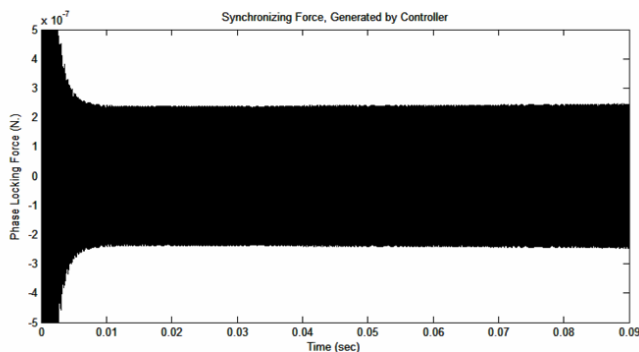

Fig. 8. Applied force profile by the controller. Maximum force generated by force balancing combs is limited to 5e-7 N.

V. CONCLUSION

This paper presented an input-output controller which was used to synchronize the output of an imperfect gyroscope with a desired model. Mechanical structure imperfections in MEMS gyroscopes resulted in unwanted energy transfer from the drive to the sense axis. Bias drift, resulted from mechanical structure imperfections, was reduced by synchronizing the output of an imperfect device with an ideal model. An input-output controller with new adaptation law was illustrated and used for accurate measurement possibilities in imperfect gyroscopes.

VI. REFERENCES

[1] B. Freidland, M. F. Hutton," Theory and Error Analysis of Vibrating-Member Gyroscope*," IEEE Transaction on Automatic Control*, vol. AC-23, no. 4, August 1978, pp. 545-556.

[2] S. Park, Adaptive Control Strategies for MEMS Gyroscopes, *PhD Dissertation* (Fall 2000) UC Berkeley Department of Mechanical Engineering.

[3] H. Xie, G. K. Fedder," Fabrication, Characterization, and Analysis of a DRIE CMOS-MEMS Gyroscope," *IEEE Journal of Sensors*, vol. 3, no. 5, October 2003, pp.662-631.

[4] C. Acar, A. M. Shkel," An Approach for Increasing Drive-Mode Bandwidth of MEMS Vibratory Gyroscopes," *IEEE Journal of Microelectromechanical Systems*, vol. 14, no. 3, June 2005, pp. 520-528.

[5] V. Annovazzi_ Lodi, R. Rajamani," Mechanical-Thermal noise in micromachined gyros," *Microelectronics Journal*, vol. 30, 1999, pp. 1227-1230.

[6] R. P. Leland, "Mechanical-Thermal Noise in MEMS Gyroscopes," *IEEE, Sensors Journal*, vol. 5, no. 3, June 2005, pp.493-500.

[7] A. Shkel, R. T. Howe, R. Horowitz, "Modeling and Simulation of Micromachined Gyroscopes in The presence of Imperfections," — online: http://www.nsti.org/publ/MSM99/W2105.pdf

[8] S. Park, R. Horowitz," Adaptive Control for the Conventional Mode of Operation of MEMS Gyroscopes," *IEEE Journal of Microelectromechanical Systems*, vol. 12, no. 1, February 2003, pp.101-108.

[9] E. J. Garcia and J. J. Sniegowski, "Surface Micro machined Microengine", *IEEE Electron Device Letters*, Vol. 17, No. 7, 366, July 1996.

[10] A. M. Shkel, R. H. Horowitz, A. A. Seshia, s. Park, R. T. Howe, " Dynamics and Control of Micromachined Gyroscopes," *American Control Conference*, San Diego, CA. Hune 1999, pp. 2119-2124.

[11] R. Horowitz, P Cheung, R.T Howe," Position sensing and control of electrostatically driven polysilicon Micro actuator,"—— P-1, P-2.

[12] G. K. Fedder, R. T Howe," Multimode Digital Control of Suspended Polysilicon Microstructure," *IEEE, Journal of Microelectromechanical systems*, vol. 5, no. 4, December 1996. pp. 283-297.

[13] W. T. Tang, M. G. Lim, R. T. Howe," Electrostatic Comb Drive Levitation and Control Method," *IEEE, Journal of Microelectromechanical systems,* vol. 1, no.4. December 1992. pp. 170-178.

[14] A. Izadian, L. A. Hornak, P. Famouri," Trajectory Control of Lateral Comb Resonators under Faulty Conditions" *American Control Conference*, New York City, NY, July 2007.

[15] A. Izadian, L. Hornak, P. Famouri," Adaptive Control of MEMS Devices" *The International Conference on Intelligent Systems and Control,* ISC 2006, August 14-16, 2006 Honolulu, Hawaii, USA.

[16] A. Izadian, P. Famouri, "On a New Input-Output Lyapunov Design Adaptive Controller," Submitted, IEEE Trans. On Control System Technology, 2008

[17] Robert P. Leland, "Adaptive Control of a MEMS Gyroscope Using Lyapunov Methods," IEEE Transaction On Control System Technology, vol. 14, no. 2, March 2006, pp 278-283